Oxygenate production from plasma-activated reaction of CO_2 and ethane

Oxygenate Production from Plasma-Activated Reaction of CO_2 and Ethane

Akash N. Biswas[†,1], *Lea R. Winter*[†,1,2,*], *Björn Loenders*[†,3], *Zhenhua Xie*[4], *Annemie Bogaerts*[3,*], *Jingguang G. Chen* [1,4,*]

1. Department of Chemical Engineering, Columbia University, New York, NY 10027, USA

2. Current address: Department of Chemical and Environmental Engineering, Yale University, New Haven, CT 06520, USA

3. Department of Chemistry, University of Antwerp, B-2610 Wilrijk, Antwerp, Belgium

4. Chemistry Division, Brookhaven National Laboratory, Upton, NY 11973, USA

Corresponding authors: leawinter@yale.edu, annemie.bogaerts@uantwerpen.be, jgchen@columbia.edu

[†] These authors contributed equally.

Abstract

Upgrading ethane with CO_2 as a soft oxidant represents a desirable means of obtaining oxygenated hydrocarbons. This reaction is not thermodynamically feasible under mild conditions and has not been previously achieved as a one-step process. Non-thermal plasma was implemented as an alternative means of supplying energy to overcome activation barriers, leading to the production of alcohols, aldehydes, and acids as well as C_1–C_{5+} hydrocarbons under ambient pressure, with a maximum total oxygenate selectivity of 12%. A plasma chemical kinetic computational model was developed and found to be in good agreement with the experimental trends. Results from this study illustrate the potential to use plasma for the direct synthesis of value-added alcohols, acids, and aldehydes from ethane and CO_2 under mild conditions.

TOC Graphic

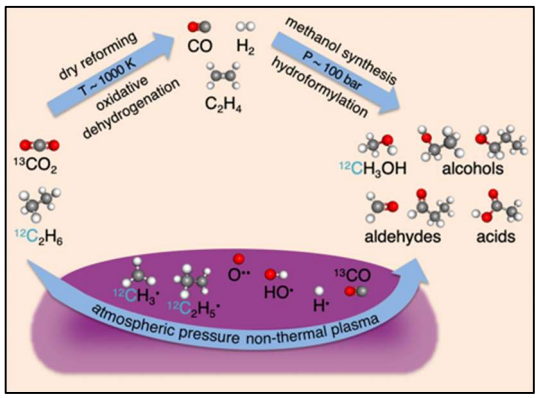

The recent abundance of shale gas has motivated efforts to upgrade light alkanes to value-added chemicals and fuels. Methane constitutes the majority of shale gas, but ethane represents up to about 10% of the gas extracted depending on the source.[1–3] Reacting ethane with CO_2 to produce value-added oxygenated hydrocarbons (such as alcohols, aldehydes, and acids) is an attractive opportunity to upgrade underutilized ethane while simultaneously reducing atmospheric CO_2 concentrations. These oxygenates can be used as versatile platform molecules for producing chemicals and fuels. At present, the production of oxygenates from ethane involves either low-efficiency, multi-step heterogeneous catalysis processes accompanied by high pressures[4,5] or homogeneous catalytic reactions that entail significant product separation challenges.[6,7] One-step conversion of ethane and CO_2 to alcohols, aldehydes, and acids under mild temperature and pressure, though, is not thermodynamically feasible. In order to circumvent thermodynamic limitations, non-equilibrium/non-thermal plasma may be employed to overcome the activation barriers of the reaction while maintaining the reactant gases near room temperature. High-energy electrons within the plasma induce vibrational/electronic excitations as well as electron impact dissociation of molecules, which can enable the formation of products that would not otherwise be produced in conventional thermochemical reactions. Furthermore, plasma-assisted oxygenate production has the potential to be of practical importance, since plasma-activated reactions are more easily adaptable to renewable electricity than are large-scale thermally-activated processes.[8,9] Modularity and fast startup/shutdown of plasma processes facilitate integration with intermittent renewable power sources or small-scale CO_2 capture.

Recently, several groups have reported plasma-assisted conversion of CO_2 with either H_2 or CH_4 to oxygenates.[10–13] Zhang et al.[14] investigated oxidative dehydrogenation of ethane with CO_2 using corona plasma, although only CO, H_2, and hydrocarbon products were detected. To our knowledge, only Gomez-Ramirez et al.[15] studied the simultaneous conversion of CO_2

and ethane using dielectric barrier discharge (DBD) plasma, but reported formaldehyde as the only oxygenated product with a vanadia/alumina catalyst dispersed on $BaTiO_3$ ferroelectric pellets. These studies have demonstrated the plasma-activated formation of oxygenates from CO_2 and methane, and of formaldehyde from CO_2 and ethane, but the steady-state production of C_2 and C_3 oxygenates, including alcohols, aldehydes, and acids, has, to our knowledge, never been reported for direct reactions of CO_2 and ethane.

In the current study, a non-thermal DBD plasma was used to demonstrate one-step multi-carbon oxygenates synthesis from ethane and CO_2. The effects of plasma power, feed gas ratio, and catalyst addition on activity and selectivity were investigated using an atmospheric pressure flow reactor based on time-on-stream results. Isotope-labeling experiments were combined with plasma chemical kinetic modeling to reveal the reaction pathways. The reaction proceeded primarily via oxidation of activated ethane derivatives by CO_2-derived oxygen-containing species, demonstrating a mechanism that is fundamentally different from thermocatalytic alcohol synthesis. The results illustrate the feasibility to use plasma to achieve the direct synthesis of oxygenates from the greenhouse gas CO_2 and underutilized ethane under ambient pressure.

The DBD flow reactor consisted of a quartz U-tube reactor equipped with an external furnace. A thermocouple served as the ground electrode, and a tantalum coil wrapped around the U-tube was connected to a plasma generator. The outlet flow was analyzed by online gas chromatography. Further details about the reactor setup can be found in the Supporting Information (Figure S1). The reactant conversion and the production of various oxygenate and hydrocarbon products were measured as a function of time during the plasma-activated reaction, as shown in Figure 1 for a 1:1 CO_2 to C_2H_6 feed ratio at 10.0 kV and 9 kHz. The C_2H_6 conversion (20.4%) was much greater than the CO_2 conversion (6.4%) (Figure 1a). CO was the main product detected, and C_1–C_{5+} hydrocarbons were also generated (Figure 1b). The main

oxygenate products detected were formaldehyde (CH_2O), 2-propanol ($CH_3CHOHCH_3$), acetic acid (CH_3COOH), ethanol (C_2H_5OH), propanal (C_2H_5CHO), propanoic acid (C_2H_5COOH), 1-propanol ($CH_3CH_2CH_2OH$), and methanol (CH_3OH) (Figure 1c).

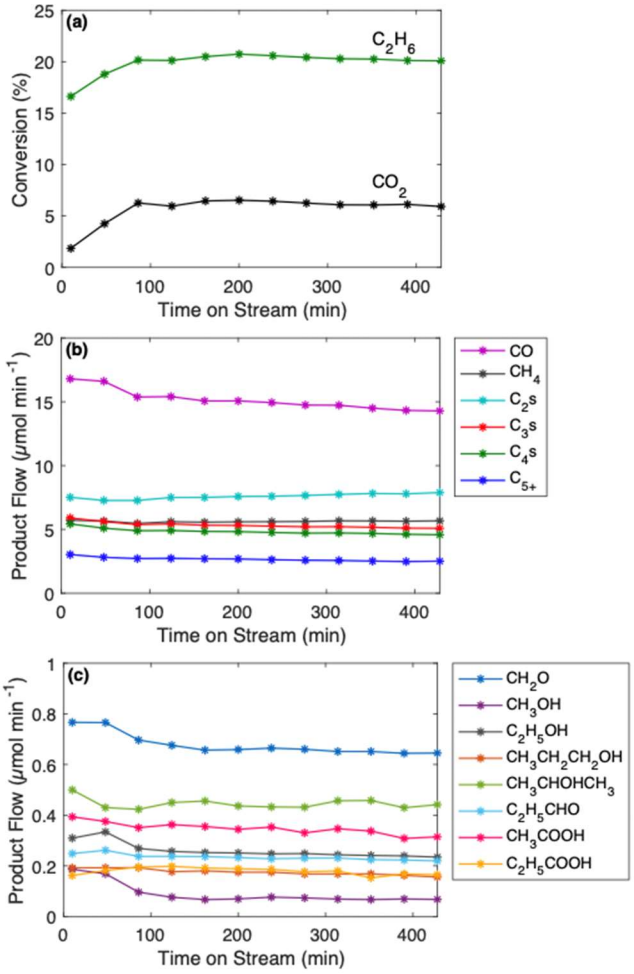

Figure 1. Conversion and product flow rates following time on stream for the reaction of CO_2 and C_2H_6 in a 1:1 feed ratio at 10.0 kV and 9 kHz under ambient pressure and 473 K. (a) Conversion of reactants, CO_2 and C_2H_6. (b) Flow rates of CO and hydrocarbon products. (c) Flow rates of oxygenate products. Reaction products were quantified using gas chromatography.

The effects of varying the feed gas ratio and plasma power on the conversion and selectivity were evaluated (Figure S2 and Figure S3). Tables S1–S3 detail the CO_2 and C_2H_6

conversions, carbon and oxygen balances, and selectivities and yields of the products. The reactant conversion increased with higher voltages, but the selectivity to oxygenate species decreased with increasing voltage. Acids were the only oxygenate products that were observed to have increased selectivity at higher voltages. Higher plasma powers also favored the production of CO, methane, and higher hydrocarbons. Further discussion about the effect of plasma power is provided by kinetic modeling below. With a higher proportion of ethane in the feed (1:2 CO_2 to C_2H_6), the selectivity to hydrocarbons was enhanced and CO production was reduced. It is evident that the formation of hydrocarbons would be favored by a greater proportion of C_2H_6 in the feed due to recombination reactions among excited hydrocarbons and radicals. Similarly, a greater proportion of CO_2 in the feed (4:1 and 9:1 CO_2 to C_2H_6) enhanced CO production relative to hydrocarbon formation. A maximum oxygenate selectivity of 12.0 ± 0.3% was achieved for a 4:1 CO_2 to C_2H_6 feed gas ratio, primarily due to the increased formaldehyde production.

The effect of adding a $RhCo_3$/MCM-41 catalyst was tested, since $RhCo_3$/MCM-41 was recently shown to be an effective heterogeneous hydroformylation catalyst, converting ethylene, CO, and H_2 to C_3 oxygenates (propanol and propanal) at 473 K.[16] Since these reactants were also produced in the CO_2 + C_2H_6 plasma reaction, the $RhCo_3$/MCM-41 catalyst was considered to be a potential candidate to enhance the production of C_3 oxygenates. When the catalyst was included, oxygenate production increased at early timescales (within 100 min of the reaction) but stabilized at a value only slightly higher than that for the plasma only experiment at longer time on stream. These results highlight the importance of dynamic changes that occur during plasma catalysis reactions, where the effects of the catalyst can change over the course of the reaction and may depend upon the timescale of the reaction. Further details and analysis regarding the plasma-catalyst tests are discussed in the Supporting Information (Figures S4–S7).

Results from flow reactor studies were used to obtain activation barriers for the reaction. Following the methods of Kim et al.[17] for plasma-assisted CH_4 dry reforming, the activation barriers, E_a, for CO_2 and C_2H_6 conversion in the flow reactor were evaluated by correlating the reaction rate with the specific energy input, SEI:

$$\frac{dA}{dt} = b \cdot e^{-\frac{E_a}{SEI}} \tag{1}$$

$$SEI = \frac{P}{F} \tag{2}$$

where dA/dt is the rate of consumption of reactant A, P is the plasma power, F is the total flow rate, and b contains pre-exponential constants. Linearization of Equation 1 enables estimation of E_a based on measuring the reaction rate with respect to plasma power at a constant flow rate:

$$\ln\left(\frac{dA}{dt}\right) = -E_a F \frac{1}{P} + b \tag{3}$$

A plot of ln(dA/dt) vs. 1/P is provided in Figure 2a for the plasma-activated reaction of CO_2 and ethane with a 1:1 feed gas ratio in the flow reactor. The linear fit of the data demonstrates that the modified Arrhenius equation holds for the plasma-activated reaction of CO_2 and ethane. The values of E_a for CO_2 and ethane were determined from the slopes in Figure 2a to be 1710 ± 350 kJ mol^{-1} (17.7 ± 3.6 eV) and 1635 ± 230 kJ mol^{-1} (16.9 ± 2.4 eV), respectively. These represent activation barriers based on the overall plasma reaction, which involve reaching the transition state and achieving bond dissociation. The reported values are on the same order of magnitude as the minimum ionization energies of CO_2 (13.3 eV) and ethane (12.7 eV), suggesting that the transition states for the plasma-activated reactions involve ionically activated forms of CO_2 and ethane. The higher CO_2 activation energy compared to ethane is also consistent with the lower CO_2 conversions observed in flow reactor experiments.

The mechanism of oxygenate formation from CO_2 and ethane was also investigated using an in situ FTIR batch reactor.[18] While the plasma properties and chemistry may be somewhat different in the batch reactor than in the flow reactor due to changes in gas transport,

electrode configuration, and He dilution ratio (see Supporting Information for experimental details), the FTIR batch reactor was employed to determine the nature of reaction intermediates. The reaction pathway was probed using ^{13}C-labeled CO_2 isotope gas in order to determine whether the C atoms in oxygenate products originated from CO_2 or ethane. As shown in the gas-phase FTIR spectra for the $^{13}CO_2$ experiments in Figure 2b, the CO product peaks at 2173 and 2116 cm^{-1} were shifted to lower frequencies, at 2121 and 2070 cm^{-1}, respectively, indicating that C atoms in CO primarily originated from CO_2. The CH_4 peak at 1304 cm^{-1} and the gas-phase ν(C–O) alcohol peak at 1028 cm^{-1} showed no shift, suggesting that the C atoms in CH_4 and alcohols were derived primarily from C_2H_6. These results imply that the mechanism for alcohol production in the current study is different from the thermocatalytic CO_2-to-alcohol reaction pathway, which involves either hydrogenation of CO_2 or CO insertion.[19–21] Rather, the plasma-activated reaction with C_2H_6 involves oxidation of ethane-derived species by O atoms derived from CO_2.

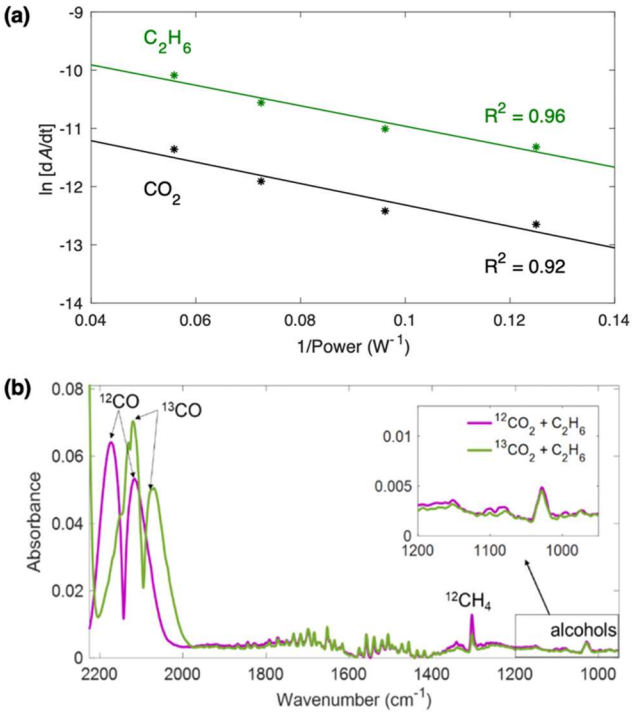

Figure 2. (a) Activation barrier measurements for the plasma-activated reaction of CO_2 and C_2H_6 using the modified Arrhenius equation with specific energy input, where reactant *A* is CO_2 or C_2H_6. (b) Gas-phase FTIR spectra of reaction products from ethane and isotope-labeled $^{13}CO_2$ (green) or $^{12}CO_2$ (magenta), which reveal no shift in the alcohol peak (1028 cm^{-1}).

To obtain further insight into the reaction pathways and trends in product distributions, chemical kinetic simulations were conducted for the reactions in the plasma using the 0D ZDPlasKin solver.[22] The model parameters (i.e., plasma power, gas temperature, applied frequency, reactor volume, and total gas flow rate) matched those of the flow reactor experiments. The species included in the model are listed in Table S4. The reaction rates were calculated from rate coefficients found in the literature or, in the case of electron impact reactions, from the electron impact cross sections and the electron energy distribution function through BOLSIG+. More information on the rate coefficients or electron impact cross sections can be found in the Supporting Information (Tables S5–S6).

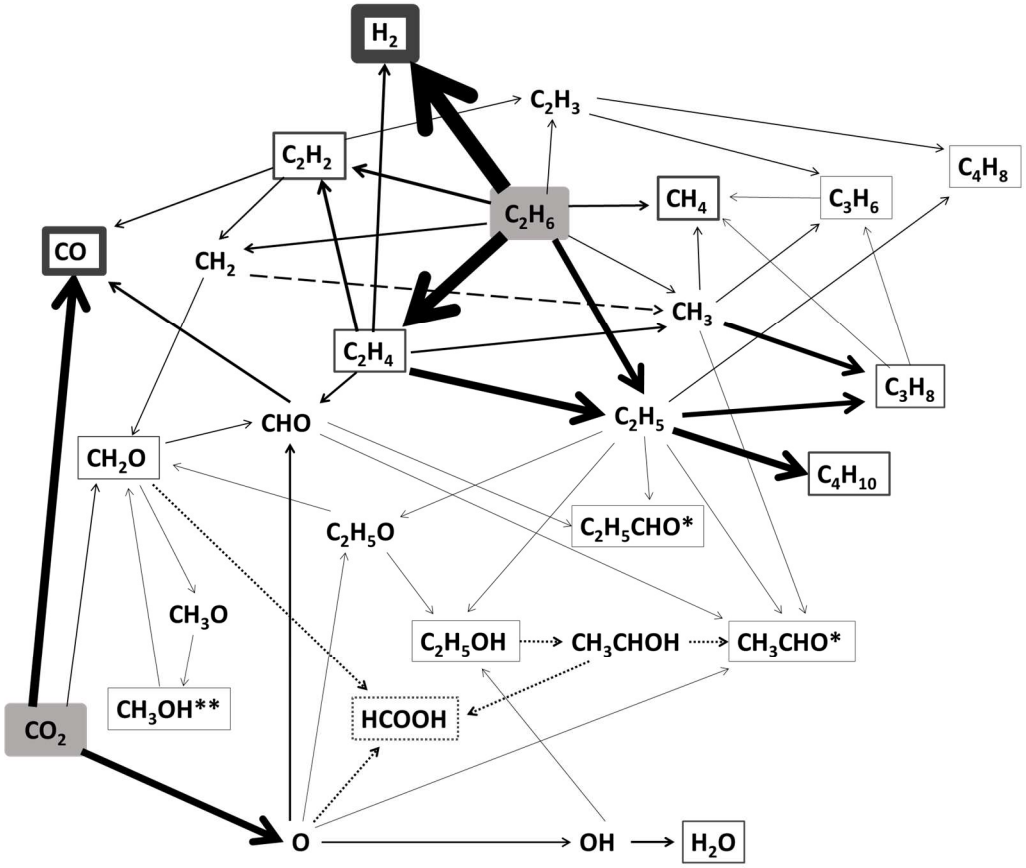

Figure 3. Schematic overview of the most important reaction pathways for the main products. The thickness of the arrows and frames indicates the importance of the corresponding pathways and product densities, respectively, with exception of the dotted lines (···) which indicate very low rates and densities. The dashed line (---) indicates an indirect pathway: $C_3H_6 + CH_2 \rightarrow C_4H_8$, followed by: $C_4H_8 + H \rightarrow C_3H_6 + CH_3$.

A schematic overview of the major reaction pathways is shown in Figure 3 as determined from the simulations. Electron impact dissociation of C_2H_6 results in the formation of stable molecules (C_2H_4, C_2H_2, CH_4, and H_2), as well as radicals (C_2H_5, CH_3, CH_2, C_2H_3, and H). The formed carbonaceous radicals react via recombination or disproportionation processes to produce longer (C_3 and C_4) hydrocarbons, or CH_4. Note that some of the formed radicals

also react back to C_2H_6. As a result of collisions with electrons, the hydrocarbon products can dissociate to produce either smaller molecules (e.g., CH_4 is formed from C_3H_6 or C_3H_8) or more unsaturated hydrocarbons (e.g., C_2H_2 and C_3H_6 are formed from C_2H_4 and C_3H_8, respectively).

Destruction of CO_2 mainly occurs via electron impact dissociation to form CO and O, and to a lesser extent through reaction with CH_2 radicals to produce CO and CH_2O. These mechanisms together are responsible for most of the CO formation, while some CO is also produced via dehydrogenation of CHO. The latter radical is formed via reaction between O radicals and C_2H_4 or through dehydrogenation of CH_2O. The CHO radical plays an important role in the formation of C_2 and C_3 aldehydes, as it recombines with CH_3 and C_2H_5 radicals, to form CH_3CHO and C_2H_5CHO, respectively. CH_3OH is mainly produced from CH_2O via CH_3O through subsequent hydrogenation reactions, while C_2H_5OH is formed via recombination of C_2H_5 with OH or O. In the latter case, subsequent hydrogenation of the resulting C_2H_5O radical forms C_2H_5OH. A more extensive overview of the main production and destruction reactions occurring in the plasma can be found in the Supporting Information.

While our model predicts direct electron impact dissociation as the main mechanism for CO_2 destruction, another possible route would be via attachment of an electron to CO_2, followed by decomposition of the CO_2^- anion to CO and O^-.[23] However, electron attachment to an isolated CO_2 molecule in the gas phase would result in a CO_2^- anion that is excited with respect to the rovibronic ground state, which would either immediately undergo electron detachment back to CO_2 or decompose into CO and O^-.[24] Therefore, our model does not include CO_2^- explicitly as separate species, but it does include electron attachment to CO_2, resulting in CO and O^- formation. However, we find that this process is not as important compared to electron impact dissociation to CO and O radicals, for the conditions achieved in our DBD plasma.

To the best of our knowledge, a detailed study regarding the reaction mechanism of CO_2/C_2H_6 reforming by plasma has not been reported before. However, the dry reforming of CH_4 in a DBD plasma has been investigated using computational modeling.[25,26] Therefore, we briefly compare the results of these studies to our results for CO_2/C_2H_6 reforming. Similar to the conversion of C_2H_6 in our study, the modeling studies by Snoeckx et al.[25] and De Bie et al.[26] predict that CH_4 destruction mainly occurs through electron impact dissociation during the microdischarge pulses. This results in the formation of CH_3 and other carbonaceous radicals, which recombine to form higher hydrocarbons. In addition, recombination between CH_3 and H radicals to again form CH_4 also occurs.[25,26] Subsequently, electron impact dissociation of the formed C_2 and C_3 hydrocarbons, and to some extent of CH_4, results in the formation of H_2.[26] This is again comparable to our case of CO_2/C_2H_6 reforming, where most H_2 is formed via electron impact dissociation of C_2H_6. The destruction of CO_2 during CH_4 dry reforming mainly occurs through electron impact reactions during the microdischarge pulses and via reaction with CH_2 radicals to form CO and CH_2O, in the afterglows in between these pulses. The latter reaction is responsible for most of the CH_2O formed, which is also the case for our results on CO_2/C_2H_6 reforming.[25,26] Hence, in general, the mechanism for the reforming of CO_2/C_2H_6 and CO_2/CH_4 in DBD plasma appear to be quite similar.

Figure 4a shows a good agreement for the reactant conversions between the experimental results and model. In both experiment and model, the C_2H_6 conversion is higher than that of CO_2. This is because dissociation of the C–H and C–C bonds in C_2H_6 is easier (i.e., higher reaction rates) than the dissociation of the C=O double bond in CO_2. The less reactive CO_2 is primarily destructed into CO, whereas the decomposition of C_2H_6 results either directly in the formation of various hydrocarbons (C_2H_4, C_2H_2, CH_4) or radicals (e.g., H, C_2H_5, CH_3, CH_2, C_2H_3) which can then form hydrocarbons, including C_2H_6, through recombination and disproportionation reactions. The conversions of both reactants also increase with increasing

plasma power, which is the result of two effects in the model. First, an increase in peak power density in the pulse leads to a higher mean electron temperature. At higher electron temperatures, more electrons reach the threshold energy required for electron impact dissociation, which are the main reactions for C_2H_6 and CO_2 conversion. Additionally, more electrons also reach the threshold energy for electron impact ionization, which leads to higher electron densities, and thus also increases the rate of electron impact reactions. Second, the number of microdischarges should increase when increasing the plasma power, as was observed experimentally by Ozkan et al.[27] This was implemented in the model by linearly increasing the number of microdischarges per half cycle (i.e., more frequent microdischarge pulses and afterglows in between them), which was also found to enhance the conversion.

Figure 4b–d shows the selectivities calculated by the model compared to experimental results for the different plasma powers. A reasonable agreement between the experimental and modeling results was obtained for CO and C_2 hydrocarbons (Figure 4b), CH_4, C_3, and C_4 hydrocarbons (Figure 4c), and oxygenates (Figure 4d). In general, the CO selectivity increased with plasma power, while the total selectivity toward hydrocarbons decreased. This is because the hydrocarbon products react further into other products or back to C_2H_6, while CO is relatively unreactive. However, the selectivities of some hydrocarbons, such as CH_4, C_3H_6, and C_4H_8, showed a slight increase as they may be partially formed from other hydrocarbon products.

For most of the oxygenate products, the simulation results can provide a mechanistic explanation for the experimental trends. The selectivities of CH_2O and C_2H_5OH decreased at higher conversion, because as the reaction proceeded further, these oxygenates were converted into CO and other oxygenates. In contrast, the selectivities of CH_3OH and C_2H_5CHO did not decrease as much with plasma power. Although CH_3OH and C_2H_5CHO were also converted into CO, the production of these species occurred largely from other products. CH_3OH was

mainly formed from CH_2O via CH_3O through subsequent hydrogenation reactions, while C_2H_5CHO was formed through the recombination of C_2H_5 and CHO. The latter CHO radical was formed by dehydrogenation of CH_2O or oxidation of C_2H_4, which is also consistent with the reaction pathway predicted by the $^{13}CO_2$ in situ FTIR experiments involving oxidation of ethane-derived hydrocarbons. Furthermore, CH_2O and C_2H_5OH were also converted into HCOOH, resulting in a higher HCOOH selectivity at higher plasma powers (Figure S8). The organic acids observed in the experiments were likely formed from C_2 or C_3 alcohols and aldehydes via a similar pathway, which would explain the higher selectivities measured with increasing plasma power, as well as the corresponding lower selectivities to alcohols and aldehydes at higher plasma power.

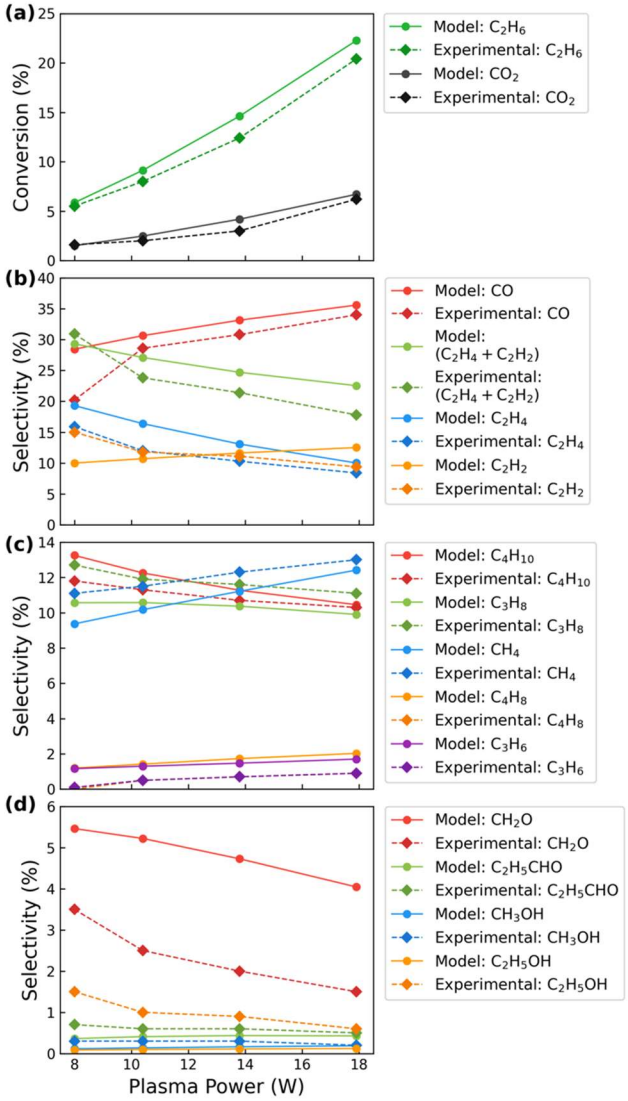

Figure 4. (a) Effect of plasma power on the reactant conversion of C_2H_6 and CO_2. Calculated and experimental selectivities for (b) CO and C_2 hydrocarbons, (c) CH_4, C_3, and C_4 hydrocarbons, and (d) oxygenates.

In summary, the current study reports, for the first time, the direct production of C_2 and C_3 alcohols, aldehydes, and acids, in addition to C_1 oxygenates, from CO_2 and ethane using non-thermal plasma at atmospheric pressure. The selectivity toward oxygenated hydrocarbon products was increased by adjusting the feed gas ratio toward higher proportions of CO_2 and by employing lower plasma powers. The inclusion of a $RhCo_3$/MCM-41 hydroformylation catalyst enhanced selectivity toward oxygenates, but only for relatively short reaction

timescales. Kinetic analysis enabled measurement of activation barriers for the plasma reaction based on the specific energy input. A detailed plasma chemical kinetic model was built to establish the major reaction pathways, which were found to be in good agreement with experimental trends. Furthermore, the kinetic modeling results were consistent with isotope-labeled measurements, which revealed a plasma reaction pathway where oxygenate formation occurred via oxidation of ethane-derived species. This study reveals a potential opportunity to apply plasma, powered by renewable energy, to convert abundant ethane from shale gas to valuable oxygenates while simultaneously utilizing CO_2 as a co-reactant.

Supporting Information Available: detailed experimental and computational procedures; additional flow reactor results; simulation parameters and list of plasma reactions

Acknowledgements

This research was supported by the U.S. Department of Energy, Office of Basic Energy Sciences, Catalysis Science Program (Grant No. DE-SC0012704). L. R. W. acknowledges the U.S. National Science Foundation Graduate Research Fellowship Program grant number DGE 16-44869. B. L. and A. B. acknowledge support from the FWO-SBO project PLASMACATDesign (grant number S001619N), as well as from the European Research Council (ERC) under the European Union's Horizon 2020 research and innovation program (grant agreement No 810182 – SCOPE ERC Synergy project).

References

(1) Yang, Yongxiang; Raipala, Kalevi; Holappa, Lauri. Ironmaking. In *Treatise on Process Metallurgy*; Elsevier Ltd., 2014; Vol. 3: Industr, pp 2–88.

https://doi.org/10.1016/B978-0-08-096988-6.00017-1.

(2) Yan, Binhang; Yao, Siyu; Kattel, Shyam; Wu, Qiyuan; Xie, Zhenhua; Gomez, Elaine; Liu, Ping; Su, Dong; Chen, Jingguang G. Active Sites for Tandem Reactions of CO_2 Reduction and Ethane Dehydrogenation. *Proc. Natl. Acad. Sci.* **2018**, *115* (33), 8278–8283. https://doi.org/10.1073/pnas.1806950115.

(3) Mimura, N.; Takahara, I.; Inaba, M.; Okamoto, M.; Murata, K. High-Performance Cr/H-ZSM-5 Catalysts for Oxidative Dehydrogenation of Ethane to Ethylene with CO_2 as an Oxidant. *Catal. Commun.* **2002**, *3* (6), 257–262.

(4) Arai, Hiromichi; Tominaga, Hiroo. Hydroformylation and Hydrogenation of Olefins over Rhodium Zeolite Catalyst. *J. Catal.* **1982**, *75* (1), 188–189.

(5) Arakawa, H.; Takahashi, N.; Hanaoka, Taka-Aki; Takeuchi, Kazuhiko; Matsuzaki, Takehiko; Sugi, Yoshihiro. Effect of Rh Dispersion on Vapor Phase and Pressurized Hydroformylation of Ethylene over Rh Catalyst. *Chem. Lett.* **1988**, *17* (11), 1917–1918.

(6) Sparta, Manuel; Børve, Knut J.; Jensen, Vidar R. Activity of Rhodium-Catalyzed Hydroformylation: Added Insight and Predictions from Theory. *J. Am. Chem. Soc.* **2007**, *129* (27), 8487–8499. https://doi.org/10.1021/ja070395n.

(7) Sivasankar, N.; Frei, H. Direct Observation of Kinetically Competent Surface Intermediates upon Ethylene Hydroformylation over Rh/Al_2O_3 under Reaction Conditions by Time-Resolved Fourier Transform Infrared Spectroscopy. *J. Phys. Chem. C* **2011**, *115* (15), 7545–7553. https://doi.org/10.1021/jp112391n.

(8) Winter, Lea R.; Chen, Jingguang G. N_2 Fixation by Plasma-Activated Processes. *Joule*

2021, *5* (2), 300–315. https://doi.org/10.1016/j.joule.2020.11.009.

(9) Bogaerts, Annemie; Neyts, Erik C. Plasma Technology: An Emerging Technology for Energy Storage. *ACS Energy Lett.* **2018**, *3* (4), 1013–1027. https://doi.org/10.1021/acsenergylett.8b00184.

(10) Wang, Li; Yi, Yanhui; Wu, Chunfei; Guo, Hongchen; Tu, Xin. One-Step Reforming of CO_2 and CH_4 into High-Value Liquid Chemicals and Fuels at Room Temperature by Plasma-Driven Catalysis. *Angew. Chemie - Int. Ed.* **2017**, *56* (44), 13679–13683. https://doi.org/10.1002/anie.201707131.

(11) Wang, Li; Yi, Yanhui; Guo, Hongchen; Tu, Xin. Atmospheric Pressure and Room Temperature Synthesis of Methanol through Plasma-Catalytic Hydrogenation of CO_2. *ACS Catal.* **2018**, *8* (1), 90–100. https://doi.org/10.1021/acscatal.7b02733.

(12) Liu, Shuang; Winter, Lea R.; Chen, Jingguang G. Review of Plasma-Assisted Catalysis for Selective Generation of Oxygenates from CO_2 and CH_4. *ACS Catal.* **2020**, *10* (4), 2855–2871. https://doi.org/10.1021/acscatal.9b04811.

(13) Li, Di; Rohani, Vandad; Fabry, Frédéric; Ramaswamy, Aravind Parakkulam; Sennour, Mohamed; Fulcheri, Laurent. Direct Conversion of CO2 and CH4 into Liquid Chemicals by Plasma-Catalysis. *Appl. Catal. B Environ.* **2020**, *261*, 118228. https://doi.org/10.1016/j.apcatb.2019.118228.

(14) Zhang, Xiuling; Zhu, Aimin; Li, Xuehui; Gong, Weimin. Oxidative Dehydrogenation of Ethane with CO_2 over Catalyst under Pulse Corona Plasma. *Catal. Today* **2004**, *89* (1–2), 97–102. https://doi.org/10.1016/j.cattod.2003.11.015.

(15) Gómez-Ramírez, Ana; Rico, Victor J.; Cotrino, José; González-Elipe, Agustín R.;

Lambert, Richard M. Low Temperature Production of Formaldehyde from Carbon Dioxide and Ethane by Plasma-Assisted Catalysis in a Ferroelectrically Moderated Dielectric Barrier Discharge Reactor. *ACS Catal.* **2014**, *4* (2), 402–408. https://doi.org/10.1021/cs4008528.

(16) Xie, Zhenhua; Xu, Yuanguo; Xie, Meng; Chen, Xiaobo; Lee, Ji Hoon; Stavitski, Eli; Kattel, Shyam; Chen, Jingguang G. Reactions of CO_2 and Ethane Enable CO Bond Insertion for Production of C_3 Oxygenates. *Nat. Commun.* **2020**, *11* (1), 1–8.

(17) Kim, Jongsik; Go, David B.; Hicks, Jason C. Synergistic Effects of Plasma-Catalyst Interactions for CH_4 Activation. *Phys. Chem. Chem. Phys.* **2017**, *19* (20), 13010–13021. https://doi.org/10.1039/c7cp01322a.

(18) Winter, Lea R.; Ashford, Bryony; Hong, Jungmi; Murphy, Anthony B.; Chen, Jingguang G. Identifying Surface Reaction Intermediates in Plasma Catalytic Ammonia Synthesis. *ACS Catal.* **2020**, *10* (24), 14763–14774. https://doi.org/10.1021/acscatal.0c03166.

(19) Xiao, Feng Shou; Ichikawa, Masaru. Catalytic Performance and Mechanism for Oxygenated Compound Formation for Ethylene Hydroformylation over Supported Ru-M Bimetallic Carbonyl Cluster-Derived Catalysts. *J. Catal.* **1994**, *147* (2), 578–593. https://doi.org/10.1006/jcat.1994.1174.

(20) Balakos, Michael W.; Chuang, Steven S. C. Dynamic and LHHW Kinetic Analysis of Heterogeneous Catalytic Hydroformylation. *J. Catal.* **1995**, *151* (2), 266–278. https://doi.org/10.1006/jcat.1995.1027.

(21) Kattel, Shyam; Ramírez, Pedro J.; Chen, Jingguang G.; Rodriguez, José A.; Liu, Ping. Active Sites for CO_2 Hydrogenation to Methanol on Cu/ZnO Catalysts. *Science* **2017**,

355 (6331), 1296–1299. https://doi.org/10.1126/science.aan8210.

(22) Pancheshnyi, S.; Eismann, B.; Hagelaar, G. J. M.; Pitchford, L. C. Computer Code ZDPlasKin. (University of Toulouse, LAPLACE, CNRS-UPS-INP, Toulouse, France). 2008.

(23) Wang, Jian-guo; Liu, Chang-jun; Eliassion, Baldur. Density Functional Theory Study of Synthesis of Oxygenates and Higher Hydrocarbons from Methane and Carbon Dioxide Using Cold Plasmas. *Energy & Fuels* **2004**, *18* (1), 148–153. https://doi.org/10.1021/ef0300949.

(24) Knapp, M.; Echt, O.; Kreisle, D.; Märk, T. D.; Recknagel, E. Formation of Long-Lived CO_2^-, N_2O^-, and Their Dimer Anions, by Electron Attachment to van Der Waals Clusters. *Chem. Phys. Lett.* **1986**, *126* (3–4), 225–231. https://doi.org/10.1016/S0009-2614(86)80074-4.

(25) Snoeckx, Ramses; Aerts, Robby; Tu, Xin; Bogaerts, Annemie. Plasma-Based Dry Reforming: A Computational Study Ranging from the Nanoseconds to Seconds Time Scale. *J. Phys. Chem. C* **2013**, *117* (10), 4957–4970. https://doi.org/10.1021/jp311912b.

(26) De Bie, Christophe; Van Dijk, Jan; Bogaerts, Annemie. The Dominant Pathways for the Conversion of Methane into Oxygenates and Syngas in an Atmospheric Pressure Dielectric Barrier Discharge. *J. Phys. Chem. C* **2015**, *119* (39), 22331–22350. https://doi.org/10.1021/acs.jpcc.5b06515.

(27) Ozkan, A.; Dufour, T.; Silva, T.; Britun, N.; Snyders, R.; Bogaerts, A.; Reniers, F. The Influence of Power and Frequency on the Filamentary Behavior of a Flowing DBD—Application to the Splitting of CO_2. *Plasma Sources Sci. Technol.* **2016**, *25* (2),

025013. https://doi.org/10.1088/0963-0252/25/2/025013.